In-situ and Laboratory Analysis of Treated Marine Soil by Consolidation Methods

Analiza in situ și de laborator a solului marin tratat prin metode de consolidare

Houssam KHELALFA. [1] [2],

1 Civil Engineering and Environment Laboratory (LGCE), University of Jijel , Algeria.
2 Department of civil engineering, Faculty of engineering and technology, Selinus university of science and literature (SUSL),   Bologna, Italy.
E-mail: khelalfahoussam@gmail.com
ORCID: 0000-0002-8052-6947

Abstract

The methods of improvement of vibroflotation (VF), dynamic compaction (DC) and the preloading took a scale in Algeria these last years, they are applied at the port of DjenDjen in Jijel province, object of our study, in the framework of its extension and its development, in order to improve the support soil which will receive the foundations of the protections structures and the container terminal in caissons. The main objective is to understand and apprehend these techniques, as well as the sensitivity of the intervening factors on its realization, and their effect on the behavior of the soil during and after its implementation. In addition, this treatment to minimize the risk of liquefaction and instability of the protective structure, However, the advantage of speed of execution and reasonable cost compared to the importance of the project, thus no negative effects have been reported on the environment. The effectiveness of these soil treatment methods has been demonstrated by the results of the available in-situ tests, in particular the SPT tests which made it possible to check the capacity of the support soil before and after its completion, as well as the settlement surveys confirm the efficiency of these techniques in terms of improving the bearing capacity of the seabed.

Keywords: Harbours, Vibroflottation, Dynamic compaction, Preloading, Soil improvement.

1. Introduction:

The construction of a port, its equipment, the layout of its access, the protection of the shoreline from the action of the sea constitute a complex set of operations, usually referred to as "maritime works" [1,2]. It was therefore quickly considered to study the mechanisms of rupture to increase their bearing capacity and eliminate settlements and risks of liquefaction [3]. Soil improvement methods are one of the tools available to the engineer to solve the stability problems or deformations he encounters when developing a project.

The dike consists of blocks or caissons of reinforced concrete, or prestressed, which with their own weight resist the forces imposed by the swell: they must be large enough to be heavy enough. When the foundation soil offers good resistance, the quays are made in the form of massive structures capable of withstanding the forces, horizontal (towards the ground, caused by the berthing of the ships and towards the basin, caused by the thrusting of embankments and mooring of ships) and vertical forces due to their own weight [1]. Ruptures are usually due either to the action of the swell or to geotechnical factors which are influenced by the self weight, the hydraulic actions and the seismic actions. There must be checks for each of these potential failure modes.

2. Consolidation methods for soil improvement:
In the feasibility study of a project, the use of soil treatment methods implies knowledge of their respective performances and limits. A question then arises: how to easily represent the application fields of each process? It has been chosen to represent the ability of a method to treat a soil according to the grain size distribution of the latter. It has the advantage of only using identification criteria obtained by simple laboratory measurements [4].

3. Analysis of Soil sample Behaviour of DjenDjen port Sites during the Laboratory tests:
The Agitation Study showed that the development of a container terminal with caisson's quay wall necessitates the extension of the protection structures (breakwaters) of the 400 m north dike and the 250 m East dike with the creation of a Groin of 100 m, to reduce the width of the entrance pass (figure 1). The protective structures adopted is of the vertical breakwater type.
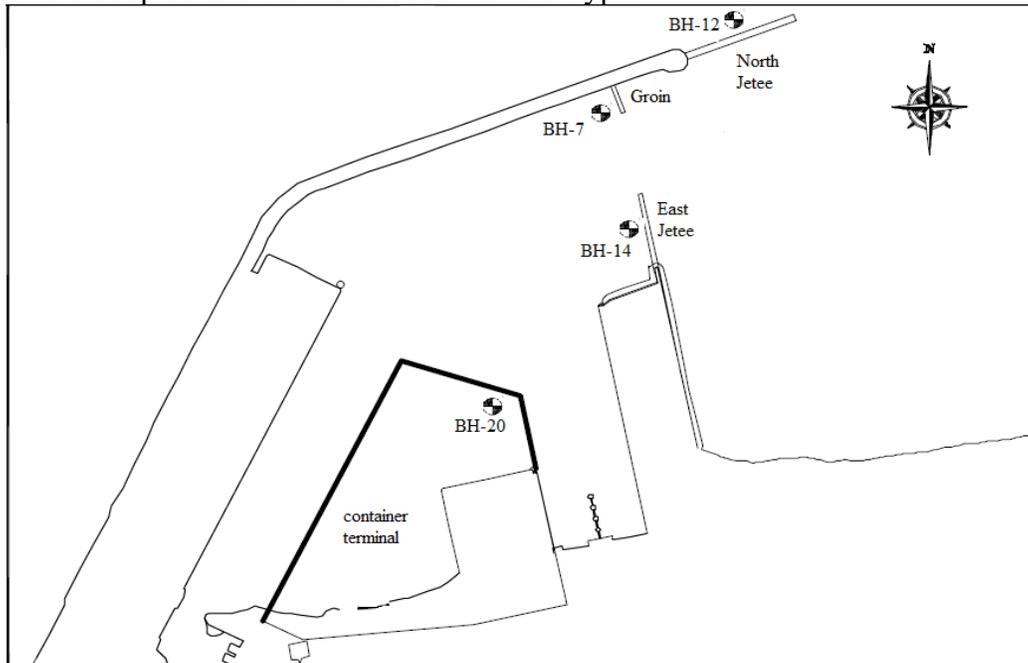

Figure-1: Ground plan of the DjenDjen port.

The purpose of this study is to verify the stability of the protective structures, as well as the quay wall of the container terminal at the port of Djen-Djen in Algeria during the extension works. To ensure the stability and strength of the foundations of the structure and to determine the effect of consolidation methods on marine soil improvement.

We conducted a drilling study, physical research and tests at the initial site on the project area; seeking to know the state of the layers on the ground base, the physical and dynamic characteristics of the soil, we conducted tests below to offer mechanical data on ground necessary during the design. We conducted a drilling study for a total of 4 wells (Figure 1) (1 hole on the north dike, 1 hole on the east dike, 1 hole on the groin, 1 hole in the container terminal section). In the dike and terminal sections, drilling was done on 5 meters of marl.

3.1 Basement conditions:

The geotechnical survey and the results of the laboratory tests showed that the soil in the study area consisted, in order and depending on the depth, of sandy and gravelly sedimentary layers and marl (Figure 2). In general, silty sand is predominant, and beneath, layers of gravel or gravelly sand are observed. In the area of the East Jetty, found among the upper layers of sand, sand mixed layers of rocks.
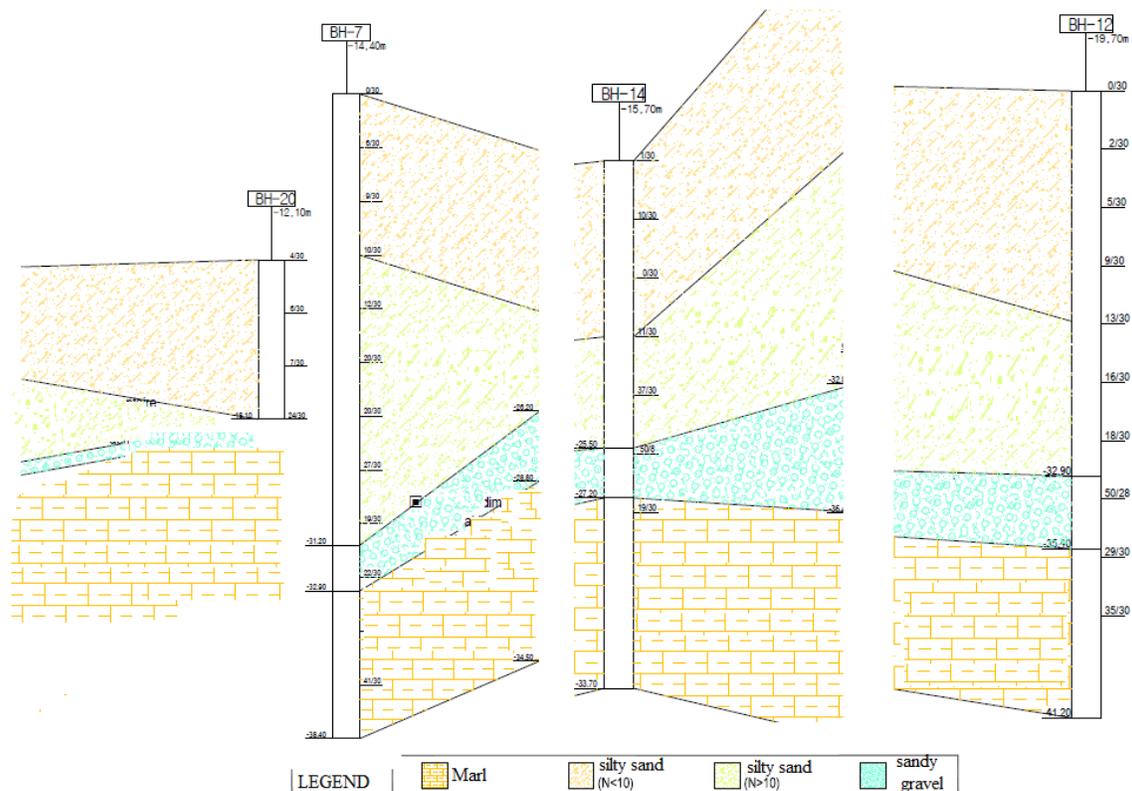

Figure-2: lithological section of the port site.

3.1.1 North Jetty (BH-12):

Figure 2 shows the cross-section of the north dike section. Based on the results of the in-situ study and laboratory tests, drilling results of 21.5 m maximum are as follows:

☐*Very loose to loose silty sand*
The upper part consists of weak silty sand of gray and brown color. This sand is 6.0 to 8.0 m (PWD -25.3m ~ -28.0m) from the surface of the seabed. The N_{SPT} is from 0 to 10/30, and the natural water content is from 24.33 to 30.19%. Located in the upper part of the sedimentary layers, this layer is considered inadequate for settlement and bearing capacity.

☐*Dense to very dense silty sand*
It is a moderately or very dense silty sand of gray and brown color below a muddy and weak sand; the thickness is 4.7 to 7.2m, and it lies at -32.2m to -33.2m of PWD. The N_{SPT} is 11 to 39/30, and the natural water content is 26.07 to 28.47%.

☐*Compact to very compact sandy gravel*
It is a thin layer of pebbles located under medium and very dense muddy sand; it lies between -34.1 and -35.7m of PWD. The N_{SPT} is very high: 50/28 to 50/18.

☐*Stiff marly*
This layer is located in the lower part according to the depth of the study, and it is of a gray or brown color. This layer appears between -34.1 and -35.7m of PWD, and has been observed up to 5.5 to 6.5 m. It is a cohesive soil corresponding to CL according to the unified classification. N_{SPT} is very high: 25 to 36/30.

Table 1: BH-12

Soil Layer	Prof.		SPT N		Density humid, γh (kN/㎥)	Cohesion Cu (kPa)	Friction Angle φ, (DEG)	Deformed Moulus E (MPa)	Velocity (m/s)		Poisson's Ratio u_d	Shear Modulus G_d (kN/㎡)	Dynamic Modulus Ed (kN/㎡)	Constrained Moduls, Kd (kN/㎡)
	GL- (m)	PWD (m)	measured	average					P-wave	S-Wave				
silty Sand (N <10)	-	- 19.7	0	4	17	5<	27	0.2	1.248	63	0.499	6.94E+03	2.08E+04	3.47E+06
	2.0	-21.7	2		17	5<	28	0.8	1.373	94	0.498	1.52E+04	4.54E+04	3.79E+06
	4.0	- 23.7	5		17	5<	29	2.0	1.462	121	0.497	2.52E+04	7.55E+04	4.20E+06
	6.0	- 25.7	9		17	5<	30	3.6	1.522	142	0.496	3.50E+04	1.05E+05	4.36E+06
silty Sand (N >10)	8.0	-27.7	13	16	18	10<	31	5.2	1.560	157	0.495	4.54E+04	1.36E+05	4.53E+06
	10	-29.7	16		18	10<	32	6.4	1.583	167	0.494	5.10E+04	1.52E+05	4.23E+06
	13.2	-32.9	18		18	10<	32	7.2	1.595	172	0.494	5.44E+04	1.63E+05	4.52E+06
Gravel	15.7	-35.4	54	60	19	5<	43	37.5	1.719	233	0.491	1.05E+05	3.14E+05	5.81E+06
Marl	16	-35.7	29	33	20	181.3	15<	13.9	1.832	276	0.488	1.56E+05	4.63E+05	6.43E+06
	18	-37.7	35		20	218.8	15<	10.6	1.861	285	0.488	1.66E+05	4.94E+05	6.86E+06
	20.5	-40.2	35		20	218.8	15<	12.8	1.861	285	0.488	1.66E+05	4.94E+05	6.86E+06

3. 1. 2 Groin (BH-7) et East Jetty (BH-14):

Figure 2 shows the cross-section of the East dike and groin section. Based on the results of the in-situ study and laboratory tests, drilling results of 28.5 m maximum are as follows:

 Very loose to loose silty sand
The entire upper part consists of low silty sand gray and brown color. This sand is 6.0 to 8.0 m (PWD -10.6m ~ -22.5m) from the seabed surface. N $_{SPT}$ is 0 to 10/30, and the natural water content is 27.28 to 41.76%. Located in the upper part of the sedimentary layers, this layer is considered inadequate for settlement and bearing capacity.

Dense to very dense silty sand
It is a moderately or very dense muddy sand of gray and brown color below a muddy and weak sand; the thickness is 3.7 to 12.6m, and it lies at -23.2m to -31.2m of PWD. N_{SPT} is 11.30 to 50/25, and the natural water content is 27.45 to 28.47%.

Compact to very compact sandy gravel
It is a thin layer of pebbles located under medium and very dense muddy sand; it lies between -27.2 and -32.9m of PWD. N_{SPT} is very high: 22/30 to 50/10.

Stiff marly
This layer is located in the lower part depending on the depth of the study, and it is a gray or brown color. This layer appears between -27.2 and -32.9m of PWD, and has been observed up to 5.5 to 7.8m. It is a cohesive soil corresponding to CL according to the unified classification. N_{SPT} is very high: 29/30 to 43/30.

Table 2: BH-14

Soil Layer	Prof. GL- (m)	PWD (m)	SPT N measured	average	Density humid, γh (kN/m³)	Cohesion Cu (kPa)	Friction Angle φ, (DEG)	Deformed Moulus E (MPa)	Velocity (m/s) P-wave	S-Wave	Poisson's Ratio u_d	Shear Modulus G_d (kN/m²)	Dynamic Modulus Ed (kN/m²)	Constrained Moduls, Kd (kN/m²)
silty Sand (N <10)	-	-15.7	1	6	17	5<	27	0.4	1.310	77	0.498	1.03E+04	3.09E+04	2.58E+06
	2.0	-17.7	10		17	5<	30	4.0	1.533	146	0.495	3.71E+04	1.11E+05	3.70E+06
	4.0	-19.7	0		17	5<	27	0.2	1.248	63	0.499	6.94E+03	2.08E+04	3.47E+06
	6.0	-21.7	11		17	5<	30	4.4	1.543	150	0.495	3.91E+04	1.17E+05	3.90E+06
silty Sand (N >10)	9.8	-25.5	37	37	18	10<	38	14.8	1.676	210	0.492	8.12E+04	2.42E+05	5.05E+06
Gravel	11.5	-27.2	188	60	19	5<	45	131.3	1.872	330	0.484	2.11E+05	6.26E+05	6.53E+06
Marl	12.0	-27.7	19	19	20	118.8	15<	81.9	1.769	257	0.489	1.35E+05	4.01E+05	6.08E+06
	15.	-30.7	19		20	118.8	15<	83.5	1.769	257	0.489	1.35E+05	4.01E+05	6.08E+06
	18.0	-33.7	19		20	118.8	15<	85.2	1.769	257	0.489	1.35E+05	4.01E+05	6.08E+06

Table 3: BH- 7

| Soil Layer | Prof. | | SPT N | | Density humid, γh (kN/m³) | Cohesion Cu (kPa) | Friction Angle φ, (DEG) | Deformed Moulus E (MPa) | Velocity (m/s) | | Poisson's Ratio u_d | Shear Modulus G_d (kN/m²) | Dynamic Modulus Ed (kN/m²) | Constrained Moduls, Kd (kN/m²) |
	GL-(m)	PWD (m)	measured	average					P-wave	S-Wave				
silty Sand (N <10)	-	-14.4	0	6	17	5<	27	0.2	1.248	63	0.499	6.94E+03	2.08E+04	3.47E+06
	2.0	-16.4	6		17	5<	29	2.4	1.480	127	0.496	2.79E+04	8.35E+04	3.48E+06
	4.0	-18.4	9		17	5<	30	3.6	1.522	142	0.496	3.50E+04	1.05E+05	4.36E+06
	6.0	-20.4	10		17	5<	30	4.0	1.533	146	0.495	3.71E+04	1.11E+05	3.70E+06
silty Sand (N >10)	8.0	-22.4	12	20	18	10<	31	4.8	1.552	154	0.495	4.34E+04	1.30E+05	4.33E+06
	10	-24.4	20		18	10<	33	8.0	1.607	177	0.494	5.77E+04	1.72E+05	4.79E+06
	12.0	-26.4	20		18	10<	33	8.0	1.607	177	0.494	5.77E+04	1.72E+05	4.79E+06
	14.0	-28.4	27		18	10<	35	10.8	1.640	193	0.493	6.82E+04	2.04E+05	4.85E+06
Gravel	16.8	-31.2	19	19	19	5<	33	13.3	1.601	175	0.494	5.92E+04	1.77E+05	4.91E+06
Marl	18.5	-32.9	22	35	20	137.5	15<	20.3	1.791	263	0.489	1.42E+05	4.22E+05	6.39E+06
	20.0	-34.4	35		20	218.8	15<	7.0	1.861	285	0.488	1.66E+05	4.94E+05	6.86E+06
	22.0	-36.4	41		20	256.3	15<	72.5	1.886	293	0.488	1.75E+05	5.21E+05	7.24E+06
	24.0	-38.4	41		20	256.3	15<	73.5	1.886	293	0.488	1.75E+05	5.21E+05	7.24E+06

3.1.3 Container terminal areas (BH-20):

To check the deeper layer, we examined 17.0m for BH-20. The layer within 6m of the upper part in the filling section is revealed as a layer of sand and weak sandy below 10 N; there is clay in the layer. Figure 2 shows the cross section of this area.

Table 4: BH-20.

| Soil Layer | Prof. | | SPT N | | Density humid, γh (kN/m³) | Cohesion Cu (kPa) | Friction Angle φ, (DEG) | Deformed Moulus E (MPa) | Velocity (m/s) | | Poisson's Ratio u_d | Shear Modulus G_d (kN/m²) | Dynamic Modulus Ed (kN/m²) | Constrained Moduls, Kd (kN/m²) |
	GL-(m)	PWD (m)	measured	average					P-wave	S-Wave				
silty Sand (N <10)	-	-5.7	3	5	17	5<	28	1.2	1.412	105	0.497	1.90E+04	5.69E+04	3.16E+06
	2.0	-7.7	7		17	5<	29	2.8	1.496	132	0.496	3.04E+04	9.10E+04	3.79E+06
	4.9	-10.6	6		17	5<	29	2.4	1.480	127	0.496	2.79E+04	8.35E+04	3.48E+06
silty Sand (N >10)	6.0	-11.7	50	21	18	10<	42	20.0	1.711	229	0.491	9.60E+04	2.86E+05	5.30E+06
	8.0	-13.7	31		18	10<	36	12.4	1.656	200	0.493	7.36E+04	2.20E+05	5.23E+06
	10.0	-15.7	16		18	10<	32	6.4	1.583	167	0.494	5.10E+04	1.52E+05	4.23E+06
	12.0	-17.7	21		18	10<	33	8.4	1.612	180	0.494	5.93E+04	1.77E+05	4.92E+06
	14.0	-19.7	20		18	10<	33	8.0	1.607	177	0.494	5.77E+04	1.72E+05	4.79E+06
	17.5	-23.2	27		18	10<	35	10.8	1.640	193	0.493	6.82E+04	2.04E+05	4.85E+06

In-situ and Laboratory Analysis of Treated Marine Soil by Consolidation Methods

Gravel	18.0	-23.7	115	89	19	5<	45	80.8	1.811	288	0.487	1.61E+05	4.79E+05	6.15E+06
	20.0	-25.7	62		19	5<	45	43.4	1.736	243	0.490	1.14E+05	3.40E+05	5.67E+06
	22.0	-27.7	125		19	5<	45	87.5	1.821	295	0.487	1.69E+05	5.01E+05	6.42E+06
Marl	24.0	-29.7	37	35	20	231.3	15<	19.8	1.870	288	0.488	1.69E+05	5.03E+05	6.99E+06
	26.0	-31.7	34		20	212.5	15<	25.2	1.857	284	0.488	1.64E+05	4.89E+05	6.79E+06
	27.8	33.5	34		20	212.5	15<	28.9	1.857	284	0.488	1.64E+05	4.89E+05	6.79E+06

The following conclusions are drawn from this investigation:
- The layers in the area of this project are of a following order: low sandy soil, medium and very dense sandy soil, marl. The weak sandy soil that is important in mechanics is 6.0 to 8.0m thick, and the N_{SPT} is less than 10/30.

- According to the results of the PDL test, the correlation with the standard penetration test is $Nd = 1.93N_{SPT}$. This correlation will help to understand the resistance after soil improvement.

- According to the results of the assessment on the possibility of liquefaction, it is expected that the liquefaction will take place in the area where the N_{SPT} is less than 10.

- According to the results of the calculation for the permitted lift according to the PDL results, it appears that the sandy and weak soil layer does not have enough lift; hence the need for soil improvement.

- The amount of immediate settlement will occur during and after the work. it will require a supervision on the settlement during the works. In general, compressive settlement takes place on the muddy and weak soil; the amount of compressive settlement will not be large for the solid marl in the area of this project. Even if the quantity is large, the time of compression is long; the amount of settlement will not be large during the life of the structures.

- Depending on the results of the liquefaction assessment and the base lift calculation, consolidation techniques are recommended. To apply these techniques requires a detailed examination of the current state of the soil; granulometry, setting the goal for soil improvement and checking for improvement effects during and after the works.
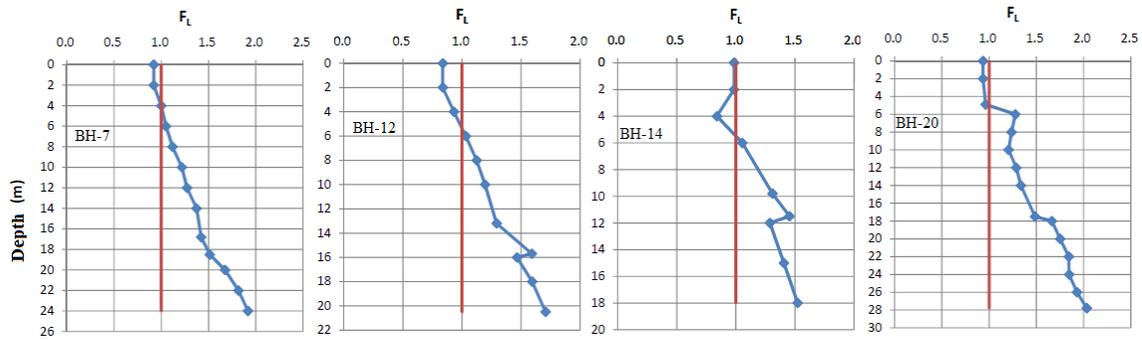
Figure 3: Liquefaction potential in different DjenDjen port areas before soil treatment.

For the detailed soil liquefaction assessment, we used the results of the standard penetration test and the vibration and triaxial compression test. As for the maximum acceleration of the surface of the earth amax, we applied 0.200g. Figure (3) shows the stability rate for liquefaction versus depth for each location. According to a detailed examination, the liquefaction is less than 1 stability rate below 10 N_{SPT}. It is therefore necessary measures against liquefaction.

3.2 Cyclic Triaxial Test:

During the study, in order to prevent the collapse of the borehole wall, an envelope was installed up to the top of the marl, and based on the speed of advance during a drilling, the condition of the silt, the color of the flowing water, samples extracted by SPT and N numbers, the layer distribution status was checked, and the order and thickness of the layers were discovered. During a standard penetration test, disturbed samples were collected by Split Spoon sampler. From the samples collected, we selected the representative sample from each layer according to the ASTM/ NF P regulations.

The cyclic triaxial test is carried out to calculate the resistance to liquefaction of the soil by including the characteristics related to the pressure and the deformation occurring on the ground during an earthquake; the earthquake deformation characteristics occurring during an earthquake are calculated by selecting the number of repetitions corresponding to the earthquake dimension. This test is used to calculate the shear stress ratio of the vibration resistance and the shear strength of the detailed liquefaction forecasting method.

Liquefaction resistance is calculated on the basis of the initial liquefaction that occurs when the effective confining pressure becomes zero; for high density sand and sandy and muddy soil, initial liquefaction does not occur; the resistance is defined according to the axial strain ratio.

3.2.1 Stress–strain behavior, failure modes, Strain energy and cyclic resistance:

A series of cyclic triaxial tests was conducted to investigate the combined effect of cyclic shear on the undrained behavior of saturated loose sand. Magnitude cycles have been imposed to simulate the responses of sand subject to cyclic loadings, and distinctly different behaviors have been observed. The excess PWP generation is one of the main concerns when assessing the liquefaction potential of sandy sites during cyclic loading. Some studies [5, 6] have shown that residual pore pressures due to plastic deformation under undrained conditions or equivalent to changes in plastic volume under drained conditions can be mathematically related to density. The cumulative energy density during deviatoric stress cycles is represented by the area of the hysteresis loop formed by a series of charges. The failure can be characterized by a large residual deformation, which differs from the flux liquefaction with a strong transient axial stress on the extension side. This type of failure with excessive accumulated cyclic stress on the compression side may be called residual deformation failure [7, 8]. A single amplitude residual deformation criterion (5%) is adopted to designate the state of failure [7, 9, 10].

 The behavior of the luminous sand with different relative density (DR-30, 50, 80) in different applied pressures, The typical effective stress path, the excess PWP generation and the axial strain with the load cycles are shown in the Figures (4-6). These tests were performed on consolidated samples with different cyclic loading modes with a CSR ranging from 0.25 to 0.4 and two different damping amplitudes (DA5%, DA10%). The sample under cyclic loading shows different responses of Figure 4 to 6, although the effective stress decreases with the number of cycles, the excess of PWP builds up moderately and stabilizes after the application of large number of cycles, and the sample does not fail with the initial liquefaction because the effective stress is always greater than zero. The development of axial deformations and its rate accelerates when the generated PWP approaches the final value. Increasing trends in axial deformation appear to be similar, also leading to failure of flow liquefaction, as evidenced by the effective stress path and stress-strain curve. Axial deformation progressively accumulates on the side of the initial static shear stress, indicating that residual deformation failure is triggered as a result of undrained cyclic loading. A similar trend with interstitial pressure responses is also seen in the figures, in which the PWP builds rapidly in the incipient loading cycles and quickly becomes stabilized with a constant end value. In addition, the cyclic loading results in the reduction of the shear modulus, which is signed by the flattened hysteresis cycle. This may be due to a decrease in the confining pressure due to the excessive pressure of interstitial water. Meanwhile, low soil resistance is not sufficient to retain liquefaction during cyclic loading. The hysteresis cycle resulting from the propagation of the wave shows that there is no insignificant reduction of the shear modulus. This indicates that the effective confining pressure is not significantly reduced due to excessive pore water pressure.

The increase in excess pore water pressure (PWP) production is shown in Figures (4-6), which indicates the gradual increase of the excess PWP ratio during cyclic loading. As shown in these Figures, the variation of the deflection stress with axial deformation (hysteresis loops) represents the degradation of the damping ratio and the shear stiffness of the soil with increasing number of loading cycles (N). During undrained cyclic loading, the rise of the PWP in saturated sand results in the reduction of intergranular forces, resulting in a reduction in soil stress and stiffness [11, 12]. The stress-strain responses of saturated samples obtained from monotonic tests at different applied loading and relative density DR are presented. It is observed that the maximum deflection stresses and the associated deformation levels are significantly affected by the variation of Confining Pressure and the relative density. In view of confining pressure, the increase in maximum deviation stress is important for increasing relative density. Therefore, it can be argued that the effect of the variation of confining pressure is greater for sands at low relative density, that is to say in the range of dense to medium-dense sands. The figures represent the exponential decay of the deviating stress with an increase of (N) which can be attributed to the deformation of the soil sample.

The distinctly different liquefaction resistance observed shows the importance of evaluating the cyclic resistance of sand under irregular loading conditions encountered in engineering proprieties. Unlike the test results of the samples with a moderate CSR, the development of axial deformations of samples with higher CSR values starts at an early stage of the stress cycles. Sufficient soil resistance provided by increasing relative density could maintain soil stability during cyclic loading. Although the results of the cyclic triaxial tests indicate that the irregularity of the load plays an important role in the cyclic behavior of sand, it has been shown that the modes of deformation and failure depend only on the type of consolidation. The following conclusions are drawn from this test:

- Two failure modes are identified for sand samples subjected to cyclic loading, namely flow liquefaction and residual deformation failure. The liquefaction of the flow occurs for the isotropically consolidated samples, accompanied by a sharp increase in pore pressure and axial strain, bringing the samples to initial liquefaction. Residual deformation failure is triggered for samples with initial static shear due to anisotropic consolidation, and failure could be defined as residual axial deformation greater than 5% on the compression side.
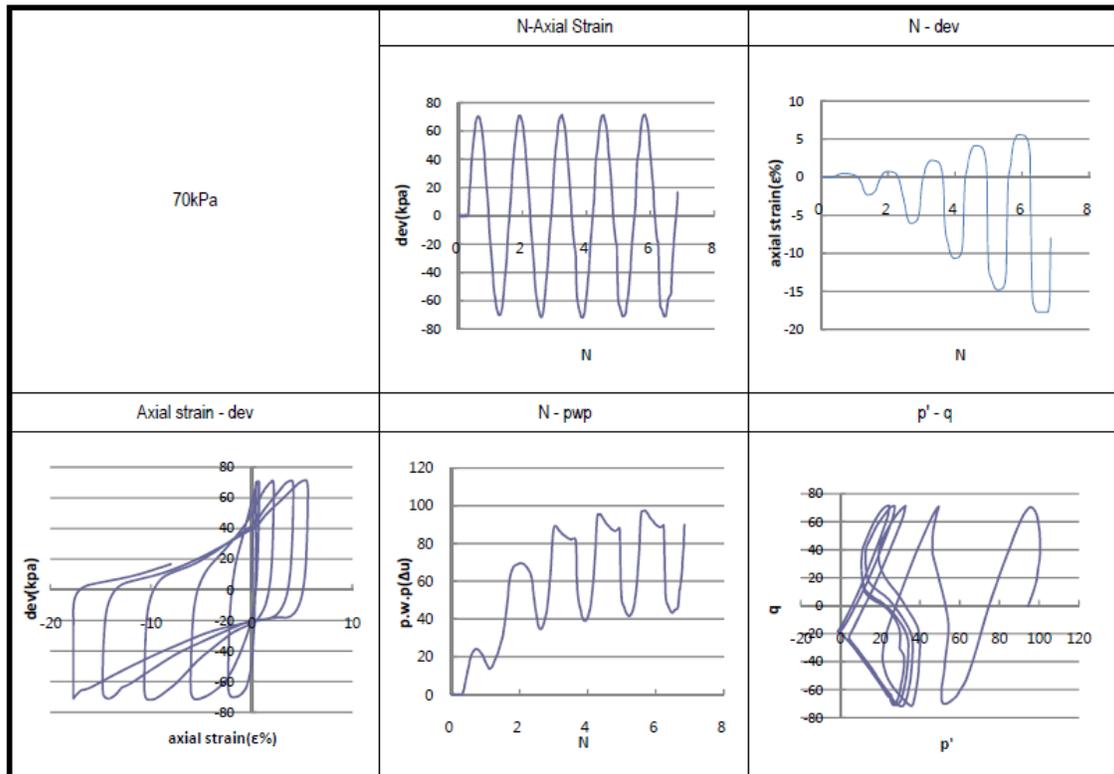
- Resistance to liquefaction of sand is greatly affected by the irregularity of the load. The results of the tests performed under load conditions indicate that the number of cycles (N) required for the failure is related to the CSR. It has been found that the presence of the initial static shear differs failures and is therefore beneficial for the cyclic resistance of the sand.

- There is a unique relationship between the residual PWP and the strain energy accumulated during the cyclic triaxial loading, irrespective of the cyclic stress

amplitude. A standardized version of the test data for pore pressure and strain energy in a narrow band suggests that the trend is independent of the loading path.

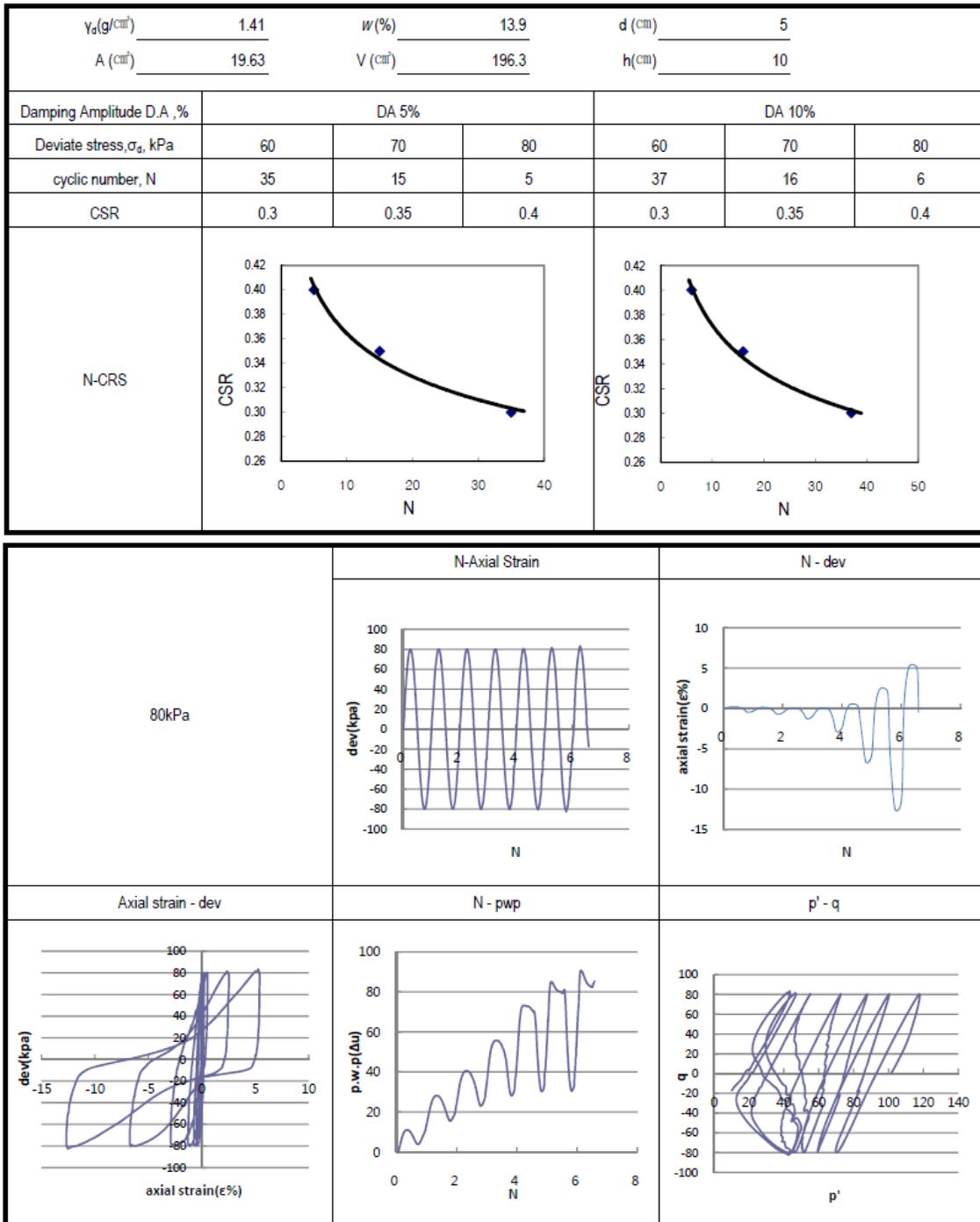| $\gamma_d(g/cm^3)$	1.33		$W(\%)$	13.9		d (cm)	5	
A (cm²)	19.63		V (cm³)	196.3		h(cm)	10	
Damping Amplitude D.A ,%	DA 5%				DA 10%			
Deviate stress,σ_d, kPa	50	60	70	50	60	70		
cyclic number, N	92	8	3	98	10	4		
CSR	0.25	0.3	0.35	0.25	0.3	0.35		

Figure 4: Cyclic response of sand (silty sand DR-30) under Cyclic loading in DjenDjen port: (a): axial strain vs N. (b) axial strain; and (c) stress- strain curve. (d) excess pore-water pressure; (e) effective stress path;

In-situ and Laboratory Analysis of Treated Marine Soil by Consolidation Methods
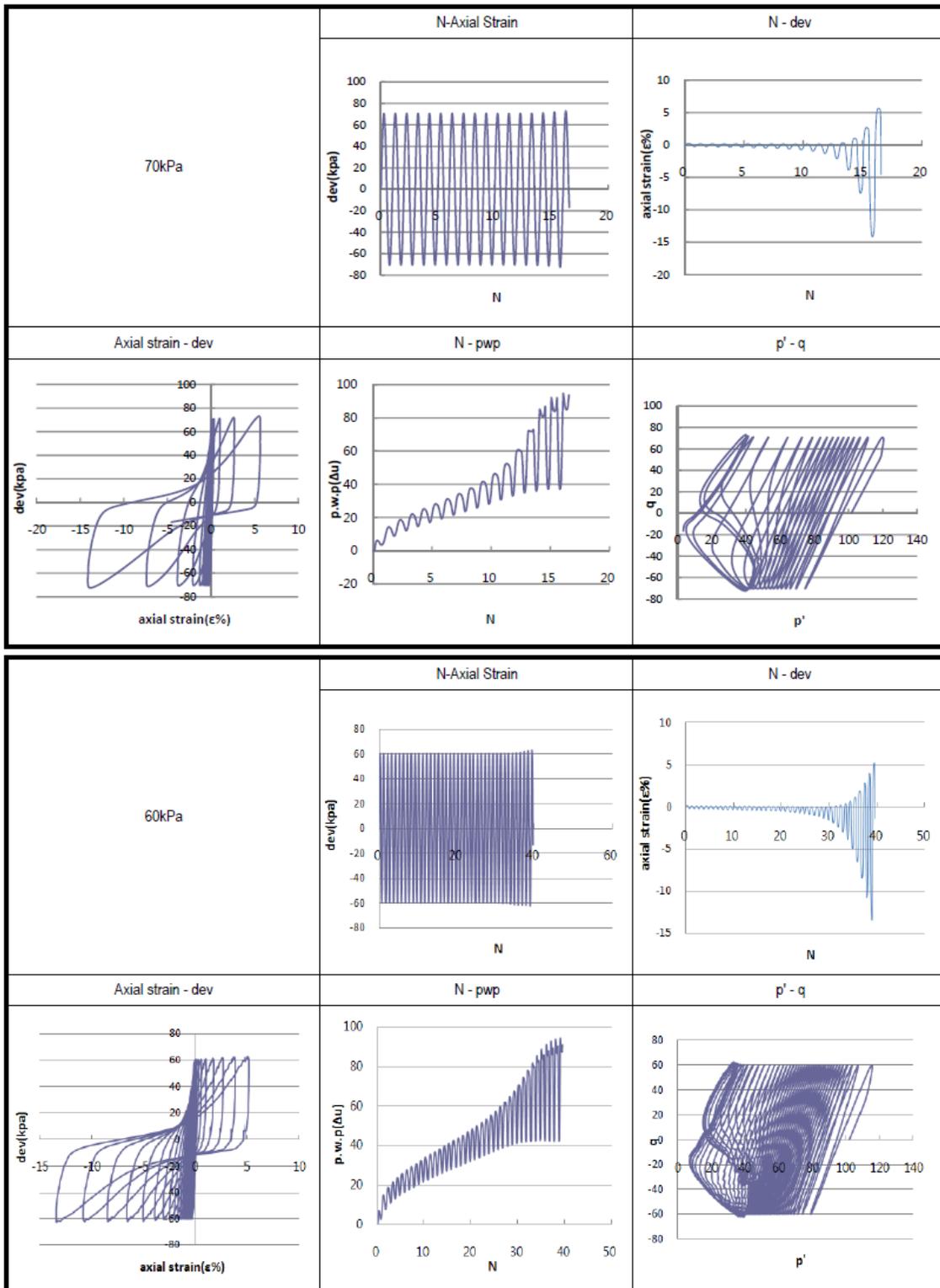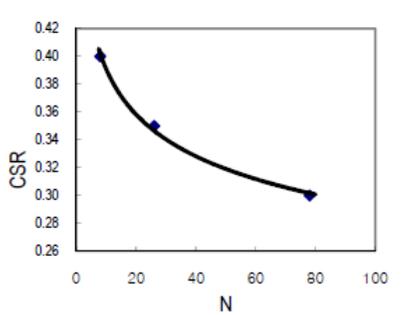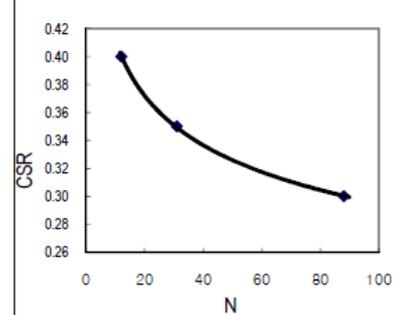
γ_d(g/cm³)	1.41		w(%)	13.9		d(cm)	5	
A(cm²)	19.63		V(cm³)	196.3		h(cm)	10	
Damping Amplitude D.A ,%	DA 5%			DA 10%				
Deviate stress,σ_d, kPa	60	70	80	60	70	80		
cyclic number, N	35	15	5	37	16	6		
CSR	0.3	0.35	0.4	0.3	0.35	0.4		

N-CRS		

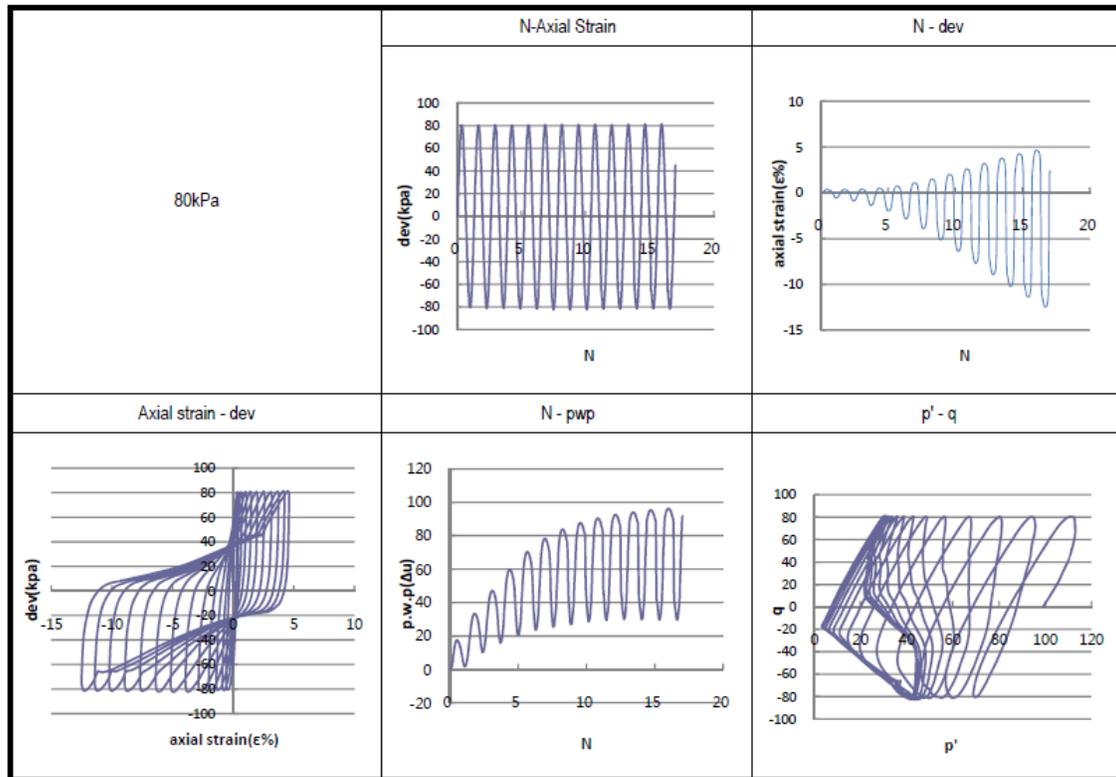|	N-Axial Strain	N - dev
80kPa		
Axial strain - dev	N - pwp	p' - q

Figure 5: Cyclic response of sand (silty sand DR-50) under Cyclic loading in DjenDjen port: (a): axial strain vs N. (b) axial strain; and (c) stress- strain curve. (d) excess pore-water pressure; (e) effective stress path;

In-situ and Laboratory Analysis of Treated Marine Soil by Consolidation Methods

γ_d(g/cm³)	1.56	W (%)	13.9	d (cm)	5
A (cm²)	19.63	V (cm³)	196.3	h(cm)	10

Damping Amplitude D.A ,%	DA 5%			DA 10%		
Deviate stress,σ_d, kPa	60	70	80	60	70	80
cyclic number, N	78	26	8	88	31	12
CSR	0.3	0.35	0.4	0.3	0.35	0.4
N-CRS						

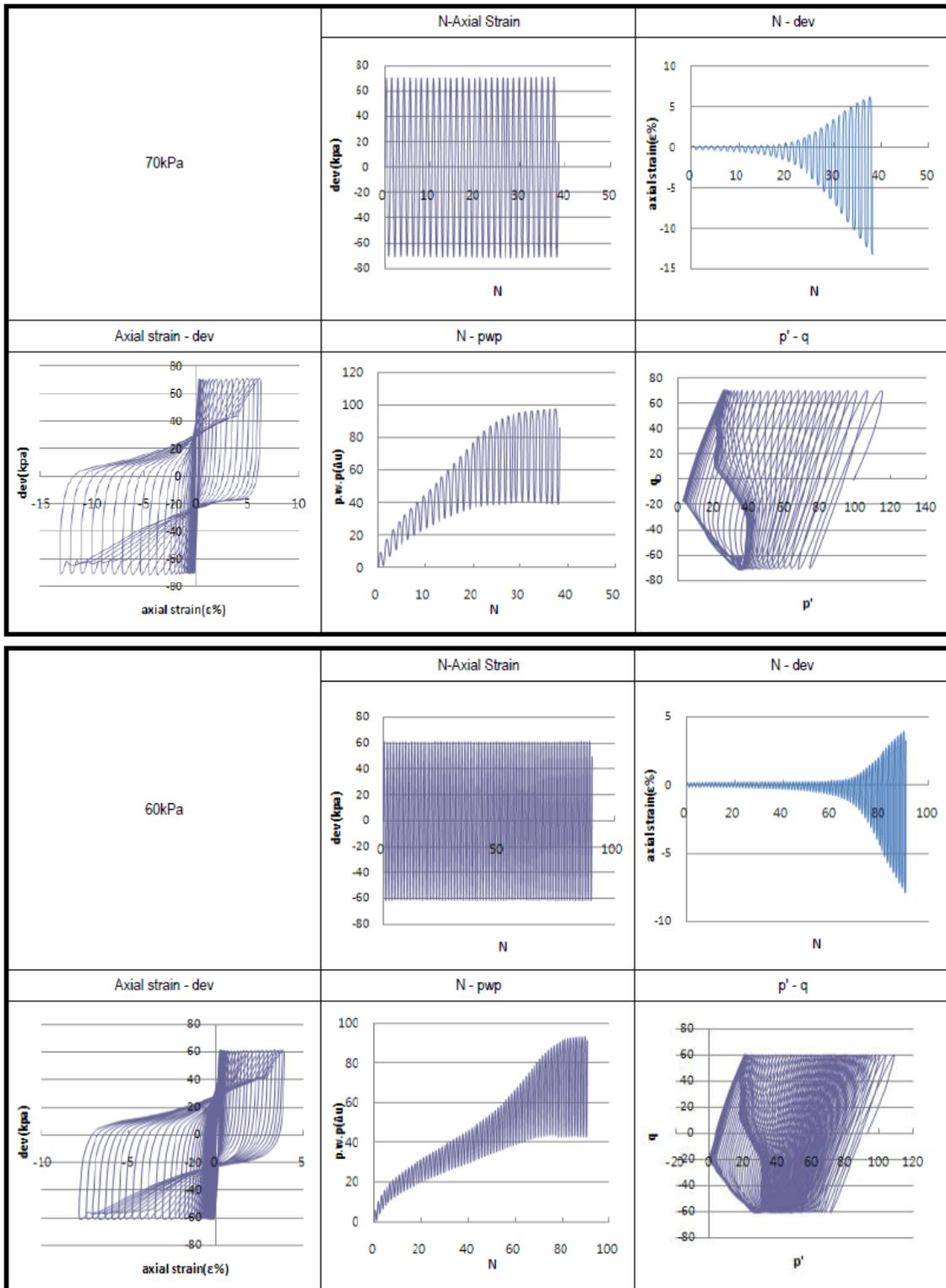|	N-Axial Strain	N - dev
80kPa		
Axial strain - dev	N - pwp	p' - q

Figure 6: Cyclic response of sand (silty sand DR-80) under Cyclic loading in DjenDjen port: (a): axial strain vs N. (b) axial strain; and (c) stress- strain curve. (d) excess pore-water pressure; (e) effective stress path.

The relative density of the original soil is on average 30% below N_{SPT} 10, and 50% above N_{SPT} 10. We have therefore carried out a test on the relative density of the original soil, and an additional test on the relative density of 80% to evaluate the stability of the liquefaction after soil improvement. Table (5) shows the results of the repetitive and triaxial compression test. As the shear stress ratio increases, the number of charges for repetitive charge required for liquefaction decreases.

Table 5: Summary of cyclic triaxial test.

Dr (%)	D .A	σ_{dev} (kPa)	CSR	N	Remarque
30 %	5 %	50	0.25	92	When N=15 CSR=0.293
		60	0.30	8	
		70	0.35	3	
50 %	5 %	60	0.30	35	When N=15 CSR=0.343
		70	0.35	15	
		80	0.40	5	
80 %	5 %	60	0.30	78	When N=15 CSR=0.372
		70	0.35	26	
		80	0.40	3	

Figure (7) shows the relationship of repetitive shear stress ratio to relative density. This ratio is a value 15 of the number of repetition of vibration corresponding to the magnitude of earthquake 7.5. As the relative density increases, the ratio of repetitive shear stress increases. These results can be applied to the assessment of liquefaction taking into account the relative density.
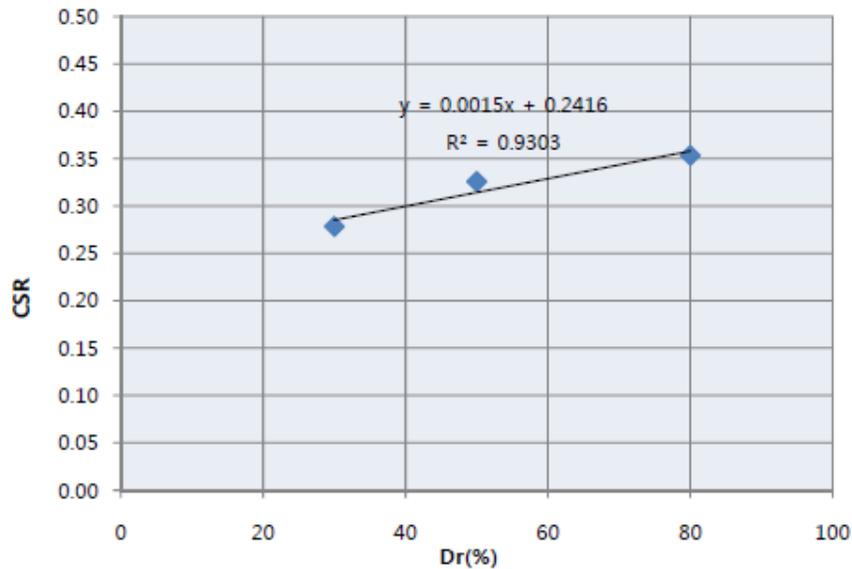

Figure 7: CSR versus relative density.

4. Vibroflotation technique (VF):

Vibroflotation is a technique for in situ densification of thick layers of loose granular soil deposits. It consists in generating, with the help of a vibrator of depth (Vibroflot), horizontal vibrations in the ground soils in order to shear them and to provoke a localized liquefaction and an immediate settlement [13,17]. Treatment with this method generally achieves the following goals: increasing bearing capacity; reduction of settlement; acceleration of consolidation; eliminating the risk of liquefaction; no adverse effects have been reported on the environment [15,16,17].

In the caisson type VII; maximum settlements of 4.7 cm were observed, settlements up to 4.9 cm for type VIII, and a maximum settlement of 8.9 cm for type V; we can see a settlements behavior in a similar way, which explains why the three (03) graphs of the settlements is almost the same, only there is a difference in settlement values, caused by the fews variation in the soil index properties. In conclusion; the results of the settlement (figure 8) are in excellent agreement with the forecasts, which reinforces our study. It is concluded that vibroflotation gives very satisfactory results in terms of soil improvement.
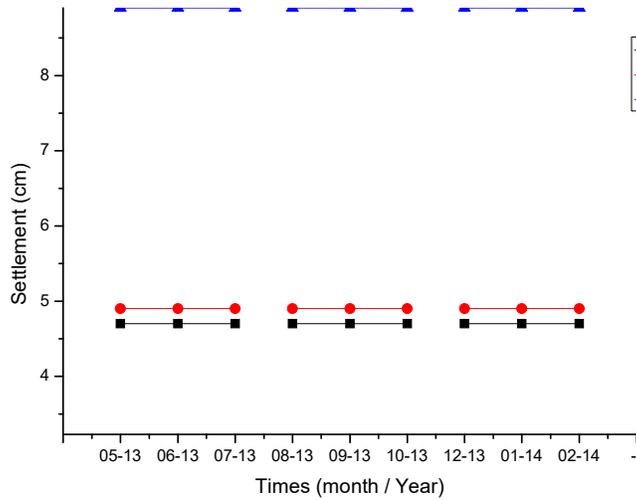
Figure 8: Comparison of settlement curves of in-situ measurements of three caissons as a function of time after soil improvement by vibroflotation.

4.1 Assessment of potential liquefaction:

The Numbers for soil design are calculated from the relational expression with the SPT N value, laboratory test results, the correlation between in-situ test results or between laboratory and in situ tests. Figure (9) and Table (6) are the results of the liquefaction test assumed after soil improvement; it takes more than 45% of the relative density improvement. If we convert it to SPT N. we get more than 15/30. So, the improved soil must be needed during 15/30.
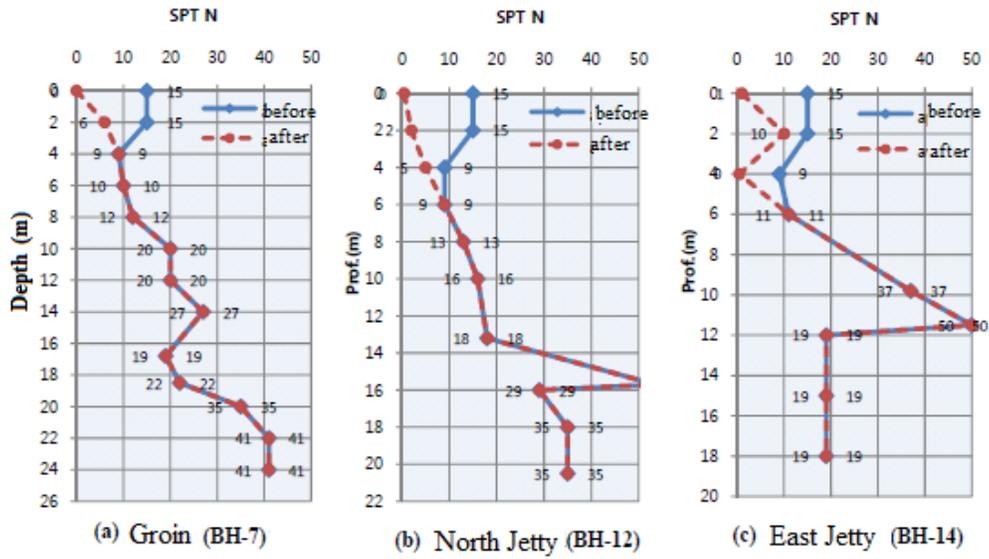
Figure 9: SPT tests before and after marine soil treatment by vibroflottation.

Table 6: Increase in relative density and decrease Liquefaction potential after treatment of seabed by vibroflotation.

Soil Layer	Prof.		SPT N	Dr (%)	Liquefaction Potnetial
	GL- (m)	PWD (m)			
BH-7	-	-14.4	15	45	NO
silty Sand (N <10)	2.0	-16.4	15	45	NO
	4.0	-18.4	9	39	NO
	6.0	-20.4	10	40	NO
BH-12	-	-19.7	15	45	NO
silty Sand (N <10)	2.0	-21.7	15	45	NO
	4.0	-23.7	9	39	NO
	6.0	-25.7	13	37	NO
BH-14	-	-15.7	15	45	NO
silty Sand (N <10)	2.0	-17.7	15	45	NO
	4.0	-19.7	9	39	NO
	6.0	-21.7	11	41	NO

5. Dynamic compaction technique (DC)

Land reclamation is generally defined as the process of creating new land by raising the elevation of a seabed, or other land at low altitude. It can be carried out by a movement of dry earth, also by hydraulic filling. Some possible failure modes in the embankment body and different failure modes need to be analyzed [18,19]. From the point of view of the foundation, this can pose a significant risk of partial or complete liquefaction and, consequently, reduction of soil resistance. Global Failure Stability Analysis provides suggestions for improvement methods to be performed.

Dynamic compaction (DC) is one of the techniques of soil improvement. It depends on the rearrangement of the soil particles using the dynamic energy produced by falling a weight (tamper) from a certain height. The concept of this technique is to improve the mechanical properties of the soil by transmitting high energy impacts on loose soils that initially have low load capacity and high compressibility potentials [20-23].

The feasibility of this technique ensure the stability of the workshop of caisson's manufacturing of the port of DjenDjen and minimize the risk of liquefaction during manufacturing. When the whole sequence of compaction has ended; the graphs of the safety factor (SF, standard and FS, on the ground from the SPT test) were presented to the liquefaction and stress distribution as a function of depth (figure 10) before and after compaction of the embankment. The results are perfectly satisfactory, which gives us the authorization to start the construction of a 1.75 m thick platform on the treated backfill, in order to install the sliding formwork and start the construction of the caissons. Since the construction of the first 1st caisson until the forty-fourth 44th; no soil settlement was noted and no geotechnical problems were encountered (Figure 11), which gives great reliability to this method of treating coastal hydraulic embankments.
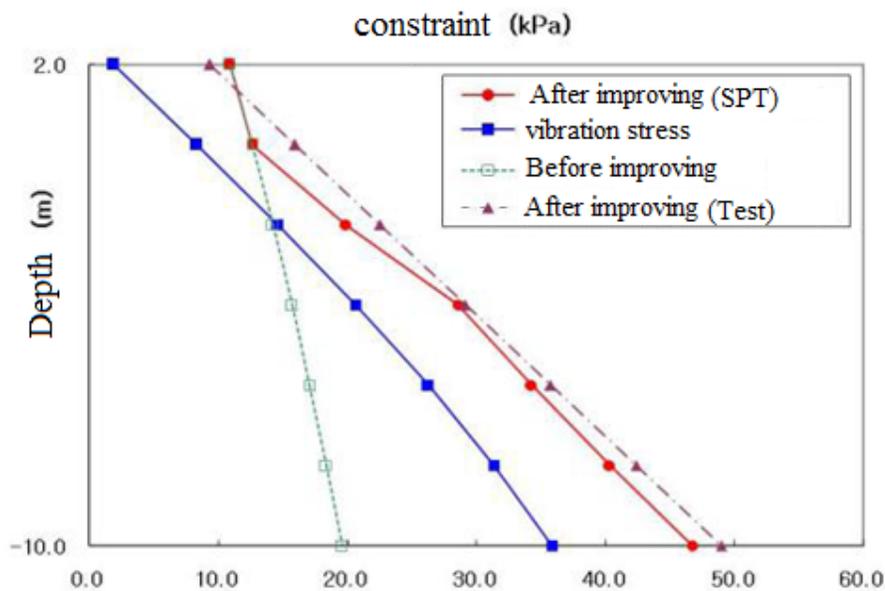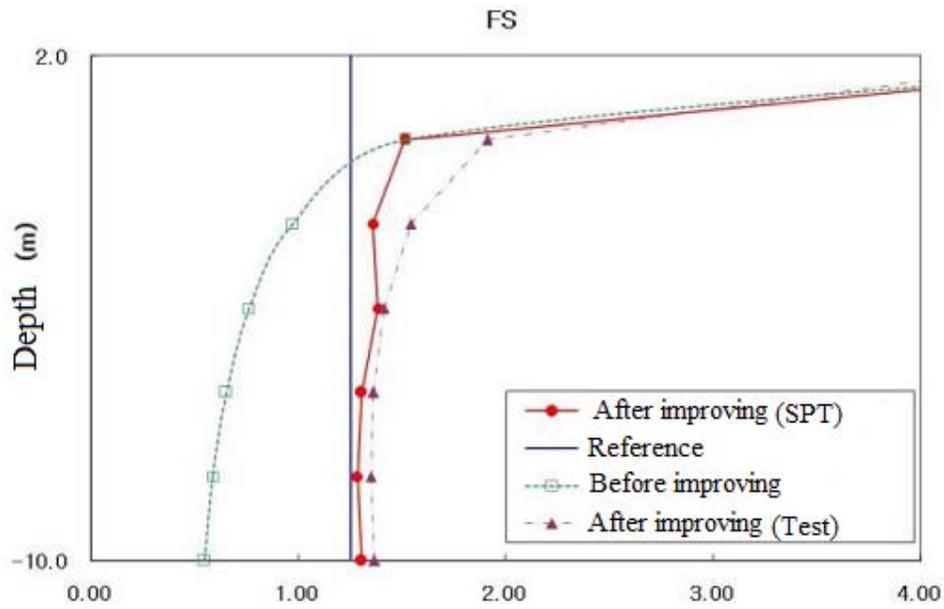
Figure 10: Safety factor (SPT) results for liquefaction and stress distribution before and after dynamic compaction.
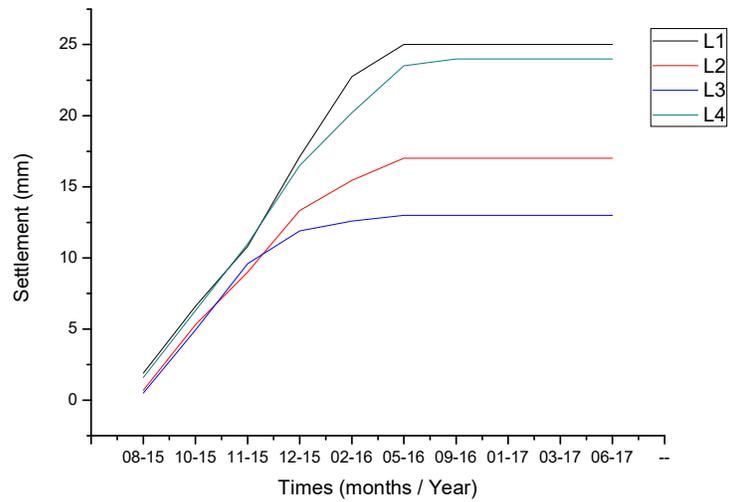

Figure 11: The results of the settlement of four (04) lines monitoring of caisson's workshop after platform implementation.

6. Pre-loading technique:

Pre-loading is a simple solution recommended for highly compressible saturated soils in order to partially accelerate their primary consolidation, which is accompanied by a reduction in settlement and as a result of an increase in undrained cohesion. When it comes to building on a saturated low lift and / or relatively compressible soil, pre-loading is the simplest technique to ensure short-term shear strength improvement [24-26].

The purpose of this study is to verify the stability of the caisson's quay walls and their foundation at the port of DjenDjen during the construction of a new container terminal. To ensure the stability and strength of the foundations of the structure and to determine the effect of the pre-loading method on the soil improvement of the foundations, the bearing capacity, the liquefaction, and settlement hazards for each profile of the foundations. Quay walls are evaluated after the completion of the work as shown in figures (12 and 13). On the basis of the AMBRASEY law and the Algerian anti-seismic standards, the examination was carried out in sections susceptible to liquefaction (sand above the layer of marly clay) in order to know if the results answer the safety factor of reference of 1.25. The results obtained according to the criteria

mentioned above confirm the liquefaction potential as a function of the depth given the weight of the quay wall, the zone where the sand layer remains corresponds to the safety factor of reference (1,25) (Figure 12).
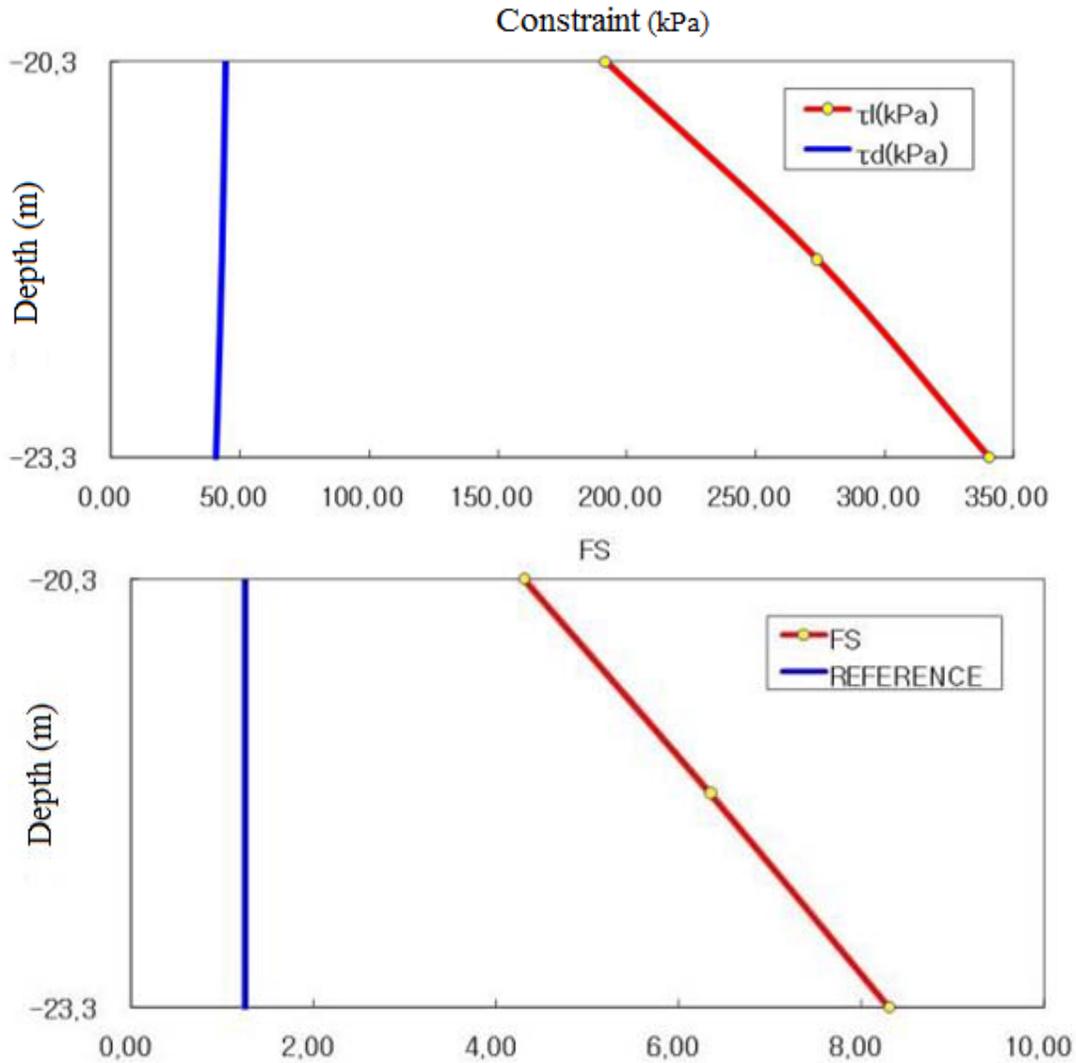

Figure 12: Safety factor (SPT) results for liquefaction and stress distribution before and after preloading.

The settlement expected during construction is 0.15 to 0.16m. A monthly settlement check of the caisson above our actual treated soil; found an average of 14.80 cm of settlement; illustrated in Figure (13). This difference in displacement is due to the effect of the soil treatment (Preloading), giving an increase in bearing capacity and an improvement of the compactness (density) of the soil which becomes denser and which has a great effect on the settlement and the deformation of the soil. Since the

removal of the preload blocks to the construction of the crown beam and its accessories (Figure 13), we have not noticed any settlement or geotechnical problems encountered, which gives the high reliability of this marine subsoil treatment method.
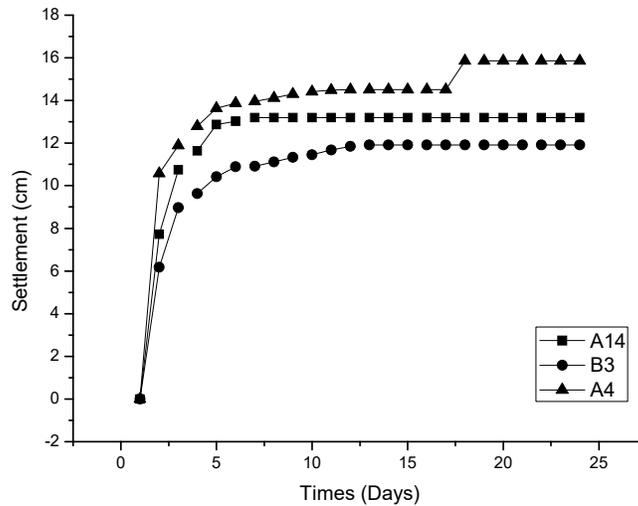

Fig. 13– Comparison of settlement curves of in-situ measurements of three caissons as a function of time during pre-loading.

7. Conclusion:

In the case where the foundation soil is particularly bad, it may be necessary to apply soil improvement measures (or other) to ensure that the structure is stable from a geotechnical perspective. Soil improvement methods should be determined only after development and analysis of the complete geotechnical companion. The three soil improvement methods used during the work of the port of DjenDjen (Algeria):

Vibroflotation, dynamic compaction and pre-loading give satisfactory results in terms of bearing capacity and reduction of the risk of liquefaction of settlements.

8. References

[1]- CIRIA – CUR – CETMEF. (2007). Therock manual. The use of rock in hydraulic engineering. 2nd edition, C683, CIRIA, London, 1304p.

[2]- BRUUNP. (1985). Design and construction of mounds for breakwaters and coastal protection. Developments in Geotechnical Engineering,Vol. 37, 1st Edition Ed. Elsevier Science, 962 p.

[3]- TERZAGHIK., PECKR.B., MESRIG. (1996).Soil mechanics in engineering practice.Ed. John Wiley & Sons, 3rd Edition, 565p.

[4]- MOSELEY M.P., KIRSCH K. (2005). Ground improvement. Ed. Taylor & Francis e-Library, 431 p.

[5]- Figueroa, J. L., A. S. Saada, L. Liang, and N. M. Dahisaria. 1994. Evaluation of soil liquefaction by energy principles. Journal of Geotechnical Engineering 120 (9):1554–69. doi:10.1061/(asce)0733–9410(1994)

120:9(1554)

[6]- Polito, C. P., R. A. Green, and J. Lee. 2008. Pore pressure generation models for sands and silty soils subjected to cyclic loading. Journal of Geotechnical and Geoenvironmental Engineering 134 (10):1490–500.

doi:10.1061/(asce)1090–0241(2008)134:10(1490).

[7]- Hyodo, M., H. Tanimizu, N. Yasufuku, and H. Murata. 1994. Undrained cyclic and monotonic triaxial behavior of saturated loose sand. Soils and Foundations 34 (1):19–32. doi:10.3208/sandf1972.34.19.

[8]- Chiaro, G., J. Koseki, and T. Sato. 2012. Effects of initial static shear on liquefaction and large deformation properties of loose saturated Toyoura sand in undrained cyclic torsional shear tests. Soils and

Foundations 52 (3):498–510. doi:10.1016/j.sandf.2012.05.008.

[9]- Ishihara, K. 1996. Soil behavior in earthquake geotechnics. Oxford:Clarendon Press.

[10]- Ishihara, K. 1993. Liquefaction and flow failure during earthquakes.Géotechnique 43 (3):351–415. doi:10.1680/geot.1993.43.3.351

[11]- Seed HB, Lee KL. Liquefaction of saturated sands during cyclic loading. Journal of the Soil Mechanics and Foundations Division 1966; 92: 105–34.

[12]- Matasovic N, Vucetic M. Cyclic characterization of liquefiable sands. Journal of Geotechnical and Geoenvironmental Engineering 1993; 119: 1805–22.

[13]- MECSIJ., GÖKALPA., DÜZCEERR. (2005). Densification of hydraulic fills by vibroflotation technique. Proceedings of the 16th International Conference on Soil Mechanics and Geotechnical Engineering, PécsUniversity, Hungary, pp 1521-1524.

[14]- GÖKALPA., DÜZCEER R. (2003).Vibratory deep compaction of hydraulic fills. Proceeding of The XIIIth European Conference on Soil Mechanics and Geotechnical Engineering, ISSMGE, Prague, Czech Republic, pp 635-638.

[15]- KELLER. (1974). Amélioration des sols (vibroflottation) Ménard. Document technique Keller, Cnam, Paris, Brochure 11-01F.

[16]- JEFFERIES M., BEEN K. (2015).Soil liquefaction, a critical state approach. CRC Press Book, 690p.

[17]- AUSSILLOUS P., COLLARTD., POULIQUENO. (2007). Liquéfaction des sols sous vagues. Proceedingdu 18ème Congrès Français de Mécanique Grenoble, 27-31 août 2007, CFM2007-0359.URL :http://hdl.handle.net/2042/16240.

[18]- VAN'T HOFF J., VAN DER KOLFF A.N. (2012). Hydraulic Fill Manual: For Dredging and Reclamation Works. Ed. CRC Press and Ed. Taylor & Francis e-Library, 672p.

[19]- USACE (2015). Dredging and dredged material management. EM 1110-2-5025, Engineering and Design, Department of the Army,U.S. Army Corps of Engineers, Washington, DC 20314-1000, USA.

[20]- HAMIDI B., NIKRAZ H., VARAKSIN S. (2009).A review on impact oriented ground improvement techniques. Australian Geomechanics Journal, Vol. 44(2), pp 17-24.

[21] K. Chow, D. M. Yong, K. Y. Yong, and S. L. Lee, "DYNAMIC COMPACTION ANALYSIS", Journal of Geotechnical Engineering. (1992) 118: 1141-1157.

[22] DimitriosZekkos, Mohammad Kabalan, and Michael Flanagan, "Lessons Learned from Case Histories of Dynamic Compaction at Municipal Solid Waste Sites", JOURNAL OF GEOTECHNICAL AND GEO-ENVIRONMENTAL ENGINEERING © ASCE / MAY 2013, DOI: 10.1061/(ASCE)GT.1943-5606.0000804.

[23] Shi-Jin Feng; Wei-HouShui; Ke Tan; Li-YaGao; and Li-Jun He, "Field Evaluation of Dynamic Compaction on Granular Deposits", JOURNAL OF PERFORMANCE OF CONSTRUCTED FACILITIES © ASCE / MAY/JUNE 2011, DOI: 10.1061/(ASCE)CF.1943-5509.0000160.

[24]- BOUASSIDA M. (2015). Amélioration des sols en place. Introduction à la géotechnique. Université Tunis El Manar, Ecole Nationale d'Ingénieurs de Tunis, Tunisie, pp 139–163.

[25]- Ramli Mohamad, PRECOMPRESSION OF SOFT SOILS BY SURCHARGE PRELOADING—SOME COMMON PITFALLS AND MISUNDERSTOOD FUNDAMENTALS, Kuala Lumpur, April 2008.

[26] - Rika Deni Susanti, Maulana and Aazokhi Waruwu; BEARING CAPACITY IMPROVEMENT OF PEAT SOIL BY PRELOADING, ARPN Journal of Engineering and Applied Sciences, VOL. 12, NO. 1, JANUARY 2017. pp 121-124.